

Computational Fluid Dynamics I

Channel Flow Problem

Gandharv Kashinath

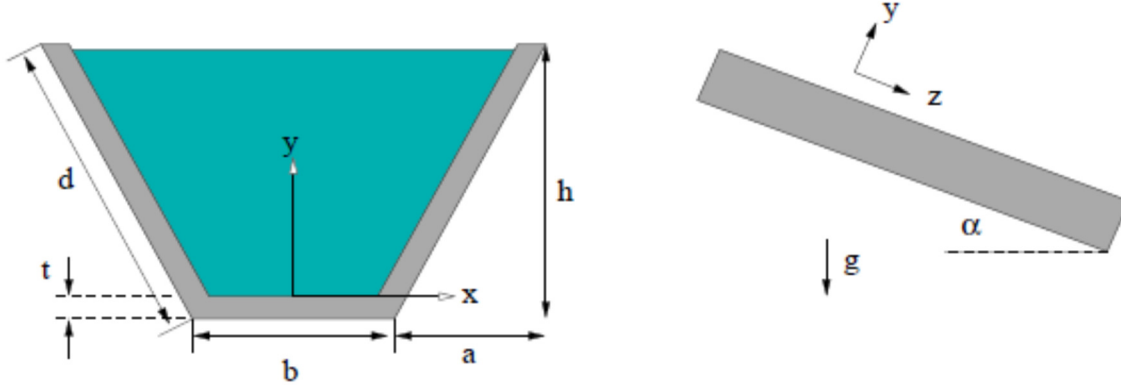
University of Michigan, Ann Arbor, MI

10/3/2008

In this project the flow through a channel was analyzed using a computational approach. The governing Poisson Equation was discretized using a finite difference approach and a computer program was written to solve the problem.

Introduction

In this project an attempt was made to solve a “Channel Flow” problem using a finite difference approach. The following figure shows the channel cross-section and side view;



The channel's wall thickness was fixed at $t=0.05$ and the cross-sectional perimeter, $l = b + 2d$, was assumed to be a constant. The channel cross section was thus parameterized in terms of two parameters: the base b and the height h .

The flow in the channel was driven by gravity, as the channel was sloped at an angle α , and by an electric field, which decays with distance from the bottom of the channel. A fully developed flow was assumed and the equations were reduced to the Poisson's equation for the velocity component, u , normal to the channel cross section,

$$-\nabla^2 u = \frac{g \sin \alpha}{\nu} + \frac{\epsilon}{\nu(y+t)^2}.$$

It was assumed that,

$$\frac{g \sin \alpha}{\nu} = 1, \quad \frac{\epsilon}{\nu} = 0.1$$

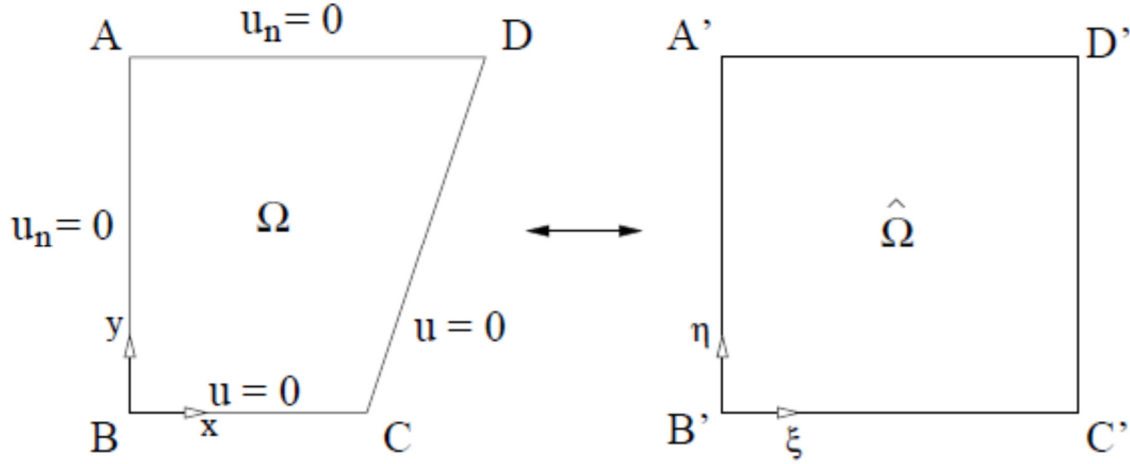
In order to implement the boundary conditions, a zero velocity condition (Dirichlet condition) was enforced along the channel walls and a zero stress condition (Neumann condition) was assumed for a free surface.

The flowrate, Q , and the power required to drive the fluid, P , were one of the main outputs chosen from the problem.

$$Q = \int_{\Phi} u \, dx \, dy, \quad P = \int_{\Phi} u^2 \frac{\epsilon}{(y+t)^2} \, dx \, dy.$$

Numerical Approach

A second order finite difference scheme was employed to solve the above problem. Making use of the symmetry, only half the channel, as illustrated below was considered. The region was mapped onto a unit square and a regular grid with $\Delta\xi = \Delta\eta = \frac{1}{N-1}$.



Results and Discussion

a) The project was initiated by deriving a mapping from the physical domain Ω (coordinates x, y) and the computational domain $\hat{\Omega}$ (coordinates ξ, η). In order to derive this transformation a Lagrange interpolation technique was used where the upper and lower boundary in the physical domain were expressed in the computational domain as follows;

For $\eta = 0$,

$$x_{\text{Lower-Bound.}} = x_1(\xi) = \frac{b}{2}\xi, \quad (1.1)$$

$$y_{\text{Lower-Bound.}} = y_1(\xi) = 0. \quad (1.2)$$

For $\eta = 1$,

$$x_{\text{Upper-Bound.}} = x_2(\xi) = \left(a + \frac{b}{2}\right)\xi, \quad (1.3)$$

$$y_{\text{Lower-Bound.}} = y_2(\xi) = h. \quad (1.4)$$

Now a Lagrange interpolation technique was used to find the various points between the two above mentioned boundaries (John C. Tannehill, 1997);

$$\vec{r}(\xi, \eta) = (1 - \eta)\vec{r}_1(\xi) + \eta\vec{r}_2(\xi), \quad \vec{r}(\xi, \eta) = \begin{bmatrix} x(\xi, \eta) \\ y(\xi, \eta) \end{bmatrix} \quad (1.5)$$

Using the above equations a mapping was obtained between the physical domain Ω (coordinates x, y) and the computational domain Ω (coordinates ξ, η) and is as follows;

$$x = \xi \left(\frac{b}{2} + \eta a \right) \xrightarrow{yields} \xi = \frac{x}{\left(\frac{b}{2} + \eta a \right)}, \quad (1.6)$$

$$y = \eta h \xrightarrow{yields} \eta = \frac{y}{h} \quad (1.7)$$

Using the above transformation the governing equations and boundary conditions were transformed into the computational domain. The $\nabla^2 u$, operator was expanded and the following expressions for the second derivatives were used;

$$u_{xx} = u_{\xi\xi} \xi_x^2 + 2u_{\xi\eta} \xi_x \eta_x + u_{\eta\eta} \eta_x^2 + u_{\xi} \xi_{xx} + u_{\eta} \eta_{xx}, \quad (2.0)$$

$$u_{yy} = u_{\xi\xi} \xi_y^2 + 2u_{\xi\eta} \xi_y \eta_y + u_{\eta\eta} \eta_y^2 + u_{\xi} \xi_{yy} + u_{\eta} \eta_{yy}. \quad (2.1)$$

By substituting the derivatives (metrics) in the above expression and simplifying terms and collecting terms the final governing equation in the computational domain was obtained as follows;

$$\frac{1}{D^2} u_{\xi\xi} + \left(\frac{\xi a}{Dh} \right)^2 u_{\xi\xi} - \left(\frac{2\xi}{Dh} \right) u_{\xi\eta} + \frac{1}{h^2} u_{\eta\eta} + \left(\frac{2\xi a^2}{D^2 h^2} \right) u_{\xi} = \frac{g \sin \alpha}{v} + \frac{\varepsilon}{v(\eta h + t)^2} \quad (2.2)$$

where;

$$D = \frac{b}{2} + \eta a \quad (2.3)$$

Finally, the boundary conditions were also transformed into the computational domain and the following expression for the Neumann boundary i.e. the north and the west boundary were obtained as follows;

North Boundary (Neumann Condition);

$$u_{\hat{n}} = u_y = 0 \xrightarrow{yields} u_{\xi} \xi_y + u_{\eta} \eta_y = 0 \xrightarrow{yields} \left(\frac{-\xi a}{Dh} u_{\xi} + \frac{1}{h} u_{\eta} \right) = 0, \quad (2.4)$$

West Boundary (Neumann Condition);

$$u_{\hat{n}} = -u_x = 0 \xrightarrow{yields} u_{\xi} \xi_x + u_{\eta} \eta_x = 0 \xrightarrow{yields} u_{\xi} = 0 \quad (2.5)$$

The Dirichlet boundary condition (i.e. $u=0$) was employed for the south and east boundaries.

b) Further second order finite difference schemes for the various derivatives were derived using a Taylor series expansion . A concise derivation of the various schemes is presented below and various applications are discussed during the derivations.

The Taylor series expansion in the ξ direction;

$$u_{i+1,j} = u_{i,j} + u'_{i,j}\Delta\xi + u''_{i,j}\frac{(\Delta\xi)^2}{2!} + u'''_{i,j}\frac{(\Delta\xi)^3}{3!} + O(\Delta\xi)^4 \quad (3.0)$$

$$u_{i-1,j} = u_{i,j} - u'_{i,j}\Delta\xi + u''_{i,j}\frac{(\Delta\xi)^2}{2!} - u'''_{i,j}\frac{(\Delta\xi)^3}{3!} + O(\Delta\xi)^4 \quad (3.1)$$

Now to find a second order finite difference scheme for the second derivative of u with respect to the ξ direction we add equation 3.0 and 3.1 to obtain;

$$u_{i+1,j} + u_{i-1,j} = 2u_{i,j} - u''(\Delta\xi)^2 + O(\Delta\xi)^4 \quad (3.2)$$

$$u''_{i,j} = \frac{u_{i+1,j} - 2u_{i,j} + u_{i-1,j}}{(\Delta\xi)^2} + O(\Delta\xi)^2 \quad (3.3)$$

Similarly, by expanding the Taylor series in the η direction and a similar procedure yields the expression for the second derivative of u with respect to the η direction and is listed below as follows;

$$u''_{i,j} = \frac{u_{i,j+1} - 2u_{i,j} + u_{i,j-1}}{(\Delta\eta)^2} + O(\Delta\eta)^2 \quad (3.4)$$

For the single derivative term a central difference scheme was employed and the scheme was obtained by subtracting equation 3.1 from 3.0 ;

$$u_{i+1,j} - u_{i-1,j} = 2u'_{i,j}(\Delta\xi) + \frac{2}{3!}u'''(\Delta\xi)^3 + O(\Delta\xi)^4 \quad (3.5)$$

$$u'_{i,j} = \frac{u_{i+1,j} - u_{i-1,j}}{(2\Delta\xi)} + O(\Delta\xi)^2 \quad (3.6)$$

This scheme was used for the North boundary in order to employ the Neumann condition.

Further, for the mixed derivative the second order central difference formula was obtained by applying central difference in both directions ξ and η as follows;

$$\frac{\partial^2 u}{\partial \xi \partial \eta} = \frac{\partial}{\partial \xi} \left(\frac{u_{i,j+1} - u_{i,j-1}}{(2\Delta\eta)} + O(\Delta\eta)^2 \right) \quad (3.7)$$

$$\frac{\partial^2 u}{\partial \xi \partial \eta} = \frac{(u_{i+1,j+1} - u_{i-1,j+1} - u_{i+1,j-1} + u_{i-1,j-1})}{(4\Delta\xi\Delta\eta)} + O(\Delta\xi)^2(\Delta\eta)^2 \quad (3.8)$$

Finally, a one sided second order scheme was also derived to be employed at the west and north boundaries. The general expression for the scheme was written as follows;

$$u'_{i,j} = \frac{au_{i,j} + bu_{i,j-1} + cu_{i,j-2}}{\Delta\eta} + O(\Delta\eta)^2 \quad (3.9)$$

The coefficients (a,b,c) are found from the Taylor series expansion of $u_{i,j-2}$ and $u_{i,j-1}$ around $u_{i,j}$.

$$u_{i,j-2} = u_{i,j} - 2u'_{i,j}\Delta\xi + u''_{i,j}\frac{(2\Delta\xi)^2}{2!} - u'''_{i,j}\frac{(2\Delta\xi)^3}{3!} + O(\Delta\xi)^4 \quad (4.0)$$

$$u_{i,j-1} = u_{i,j} - u'_{i,j}\Delta\xi + u''_{i,j}\frac{(\Delta\xi)^2}{2!} - u'''_{i,j}\frac{(\Delta\xi)^3}{3!} + O(\Delta\xi)^4 \quad (4.1)$$

Now, multiplying equation by c, equation by b and adding to $au_{i,j}$, leads to;

$$au_{i,j} + bu_{i,j-1} + cu_{i,j-2} = (a + b + c)u_{i,j} - (\Delta\xi)(b + 2c)u'_{i,j} + \left(\frac{(\Delta\xi)^2}{2}\right)(b + 4c)u''_{i,j} + O(\Delta\xi)^3 \quad (4.2)$$

and identifying three conditions from the above equation as follows;

$$\begin{aligned} a + b + c &= 0 \\ (b + 2c) &= -1 \\ b + 4c &= 0 \end{aligned} \quad (4.3)$$

Gives us the second order one sided backward difference scheme to be employed at the north Boundary for the derivative of u with respect to η ;

$$u'_{i,j} = \frac{3u_{i,j} - 4u_{i,j-1} + u_{i,j-2}}{(2\Delta\eta)} + O(\Delta\eta)^2 \quad (4.4)$$

Similarly a second order one sided forward difference scheme to be employed at the west Boundary, derivative of u with respect to ξ can be obtained and is listed as follows;

$$u'_{i,j} = \frac{-3u_{i,j} + 4u_{i-1,j} - u_{i-2,j}}{(2\Delta\xi)} + O(\Delta\xi)^2 \quad (4.5)$$

In order to evaluate the Power and the flowrate an integration procedure was employed. The power and flow rate equations were transformed into the computational domain using the Jacobian matrix as follows;

$$Q = \int_{\phi} u dx dy = \int_{\Omega} u J d\xi d\eta, \quad (4.6)$$

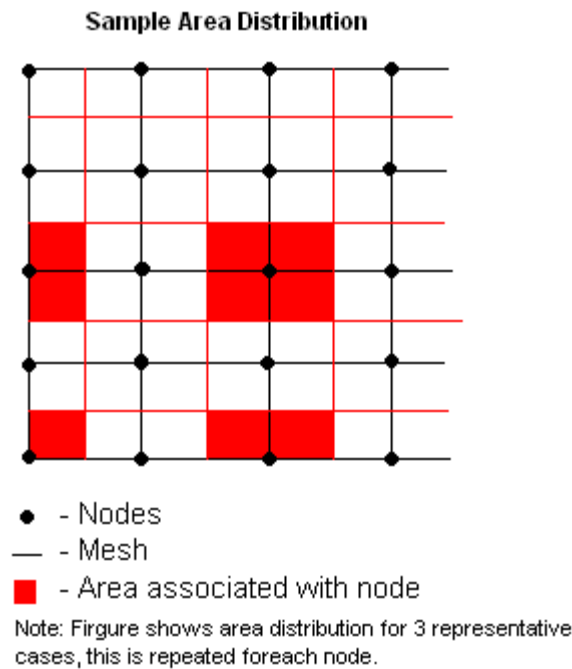
$$P = \int_{\phi} u^2 \frac{\varepsilon}{(y+t)^2} dx dy = \int_{\Omega} u^2 \frac{\varepsilon}{(y+t)^2} J d\xi d\eta. \quad (4.7)$$

October 3, 2008

where;

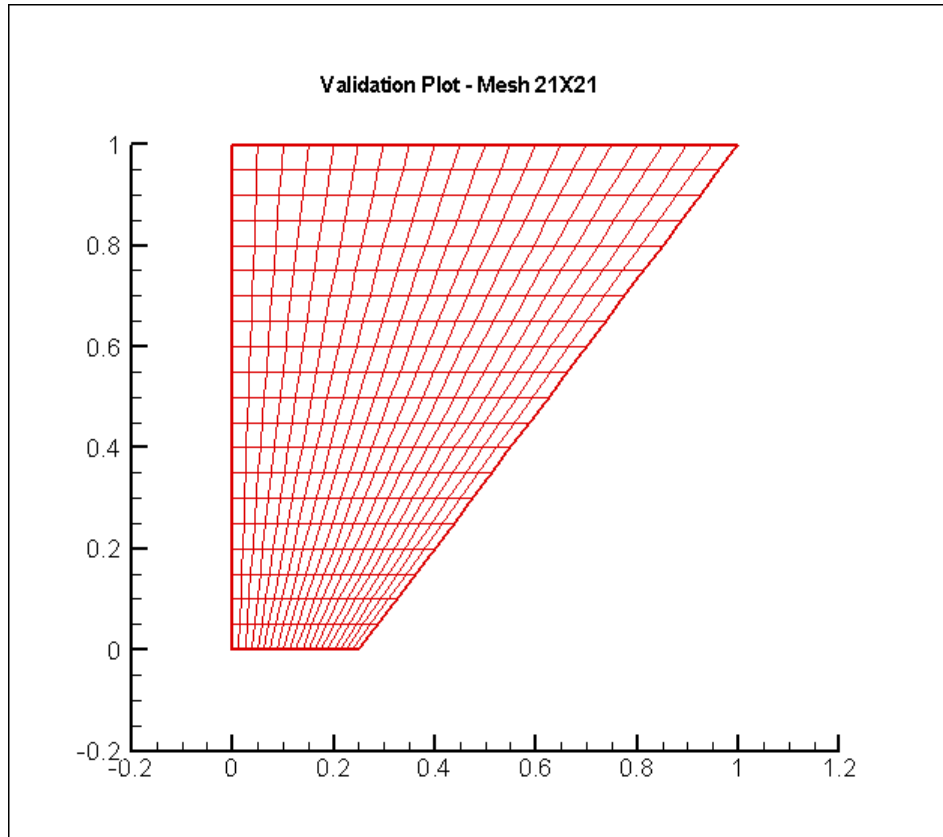
$$J = x_{\xi}y_{\eta} - y_{\xi}x_{\eta} \quad (4.8)$$

Now in order to perform the above integration a differential area was constructed around each node point and was multiplied with the u or the u^2 term accordingly. The contribution from each node was added and the final power and flow rate was provided as the output. Care was taken at the boundaries while discretizing the areas as only a 0.25 contribution was accounted for at the 4 corners and 0.5 contribution at other points on the boundary. The figure below demonstrates the area splitting as employed in the code to calculate the power and flowrate;

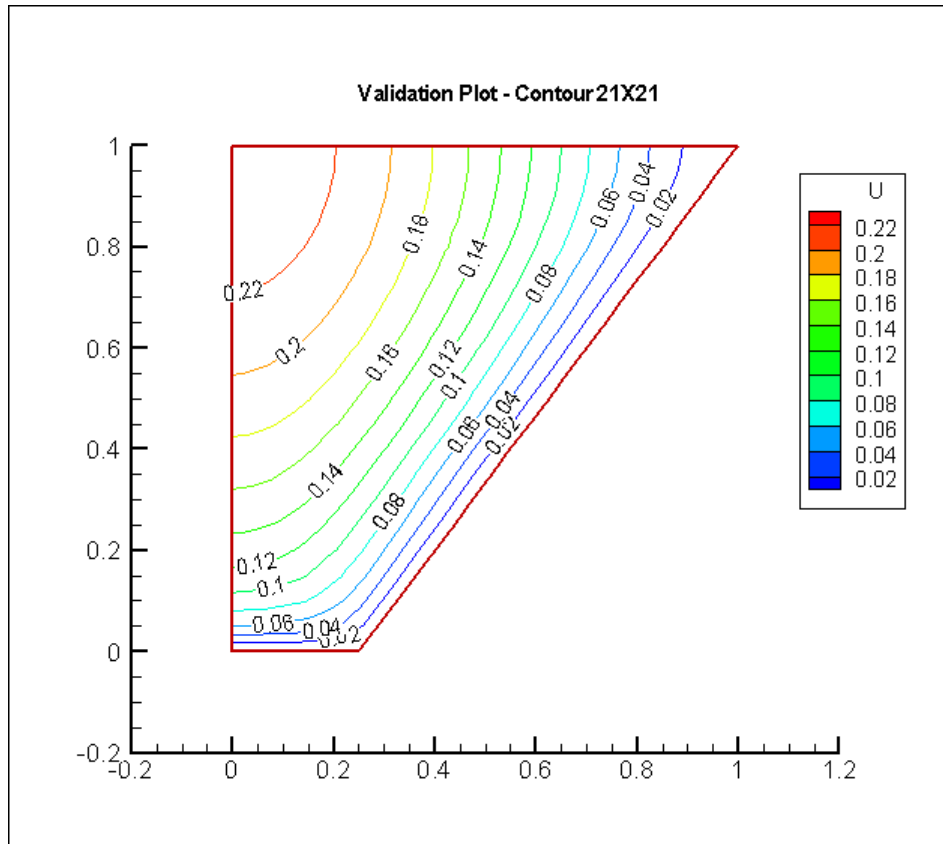


October 3, 2008

c) A computer program was constructed in FORTRAN to solve this problem. The system of linear equation obtained from the code was solved using a gaussian elimination based solver. The code was validated with the validation plots given in the project statement and the following plot for the grid with $N=21$, and the velocity distribution was obtained for $l=3.0$, $b=0.5$, and $h=1.0$;



October 3, 2008



The power and flow rate obtained from the program were as follows;

```
Power, P= 8.406539659902214E-003
Mass Flow Rate, Q= 0.155395298729111
```

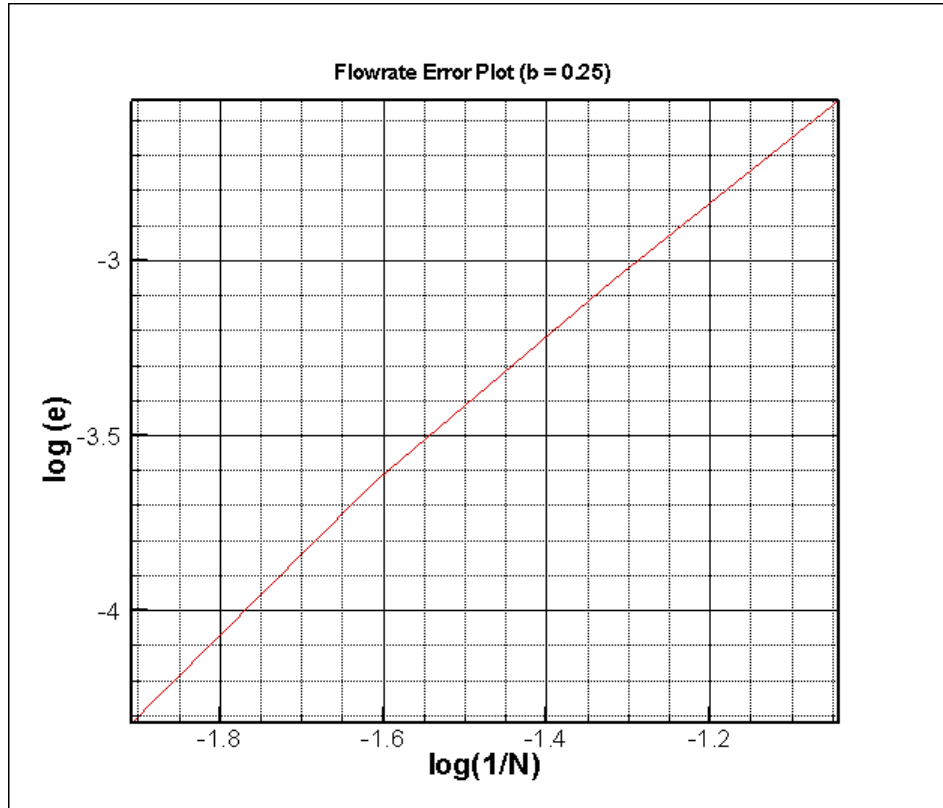
d) Further, a grid refinement study was performed to calculate the convergence rate for the errors in \hat{Q} , \hat{P} , and for the L_2 and L_∞ norms of the solution error. The code was run for mesh sizes 11, 21, 41, 81 and the solutions from these grids were interpolated to 161 by 161 grid following which the errors were calculated. The convergence rates were calculated by extracting the equation from a linear fit of the error plots in Tecplot. From the linear fit it was noted that the slope of the curve represented the convergence rate and the following results were obtained;

Convergence Rate	b = 0.25	b = 0.75
Power	1.968	1.972
Massflow	2.051	2.011
L_2 Norm	1.982	2.000
L_∞ Norm	1.329	1.564

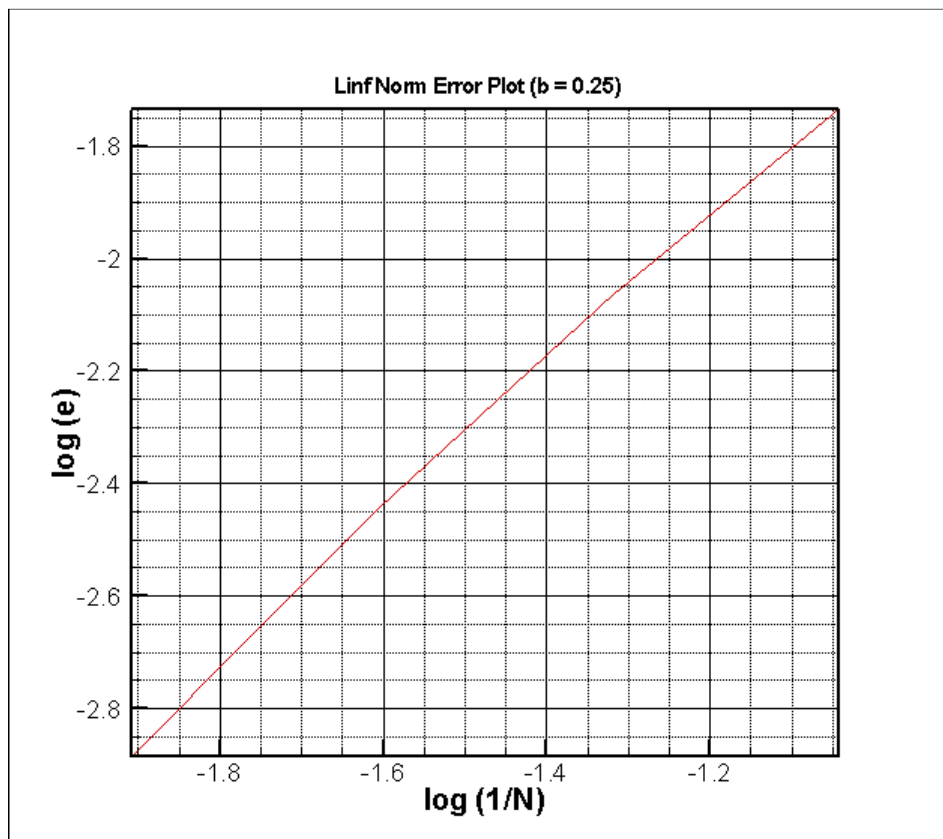
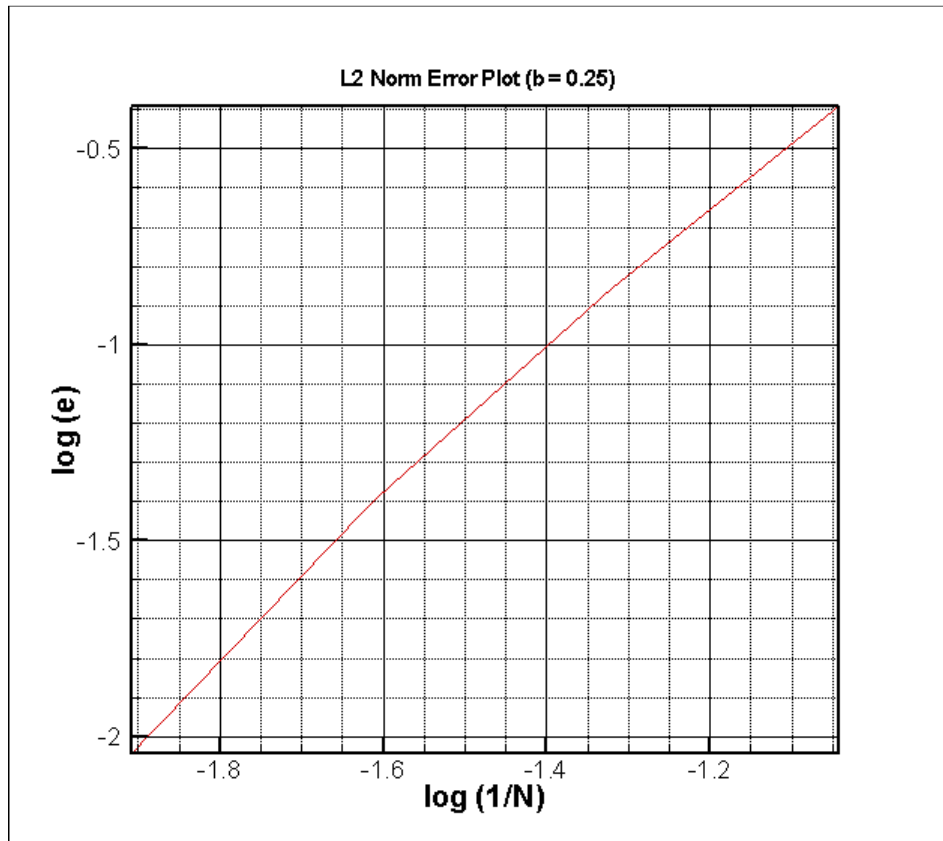
Presented below are the error plots for each of the four errors and for the two prescribed dimensions of the channel;

October 3, 2008

- $l=3.0, h=1.0, b=0.25$

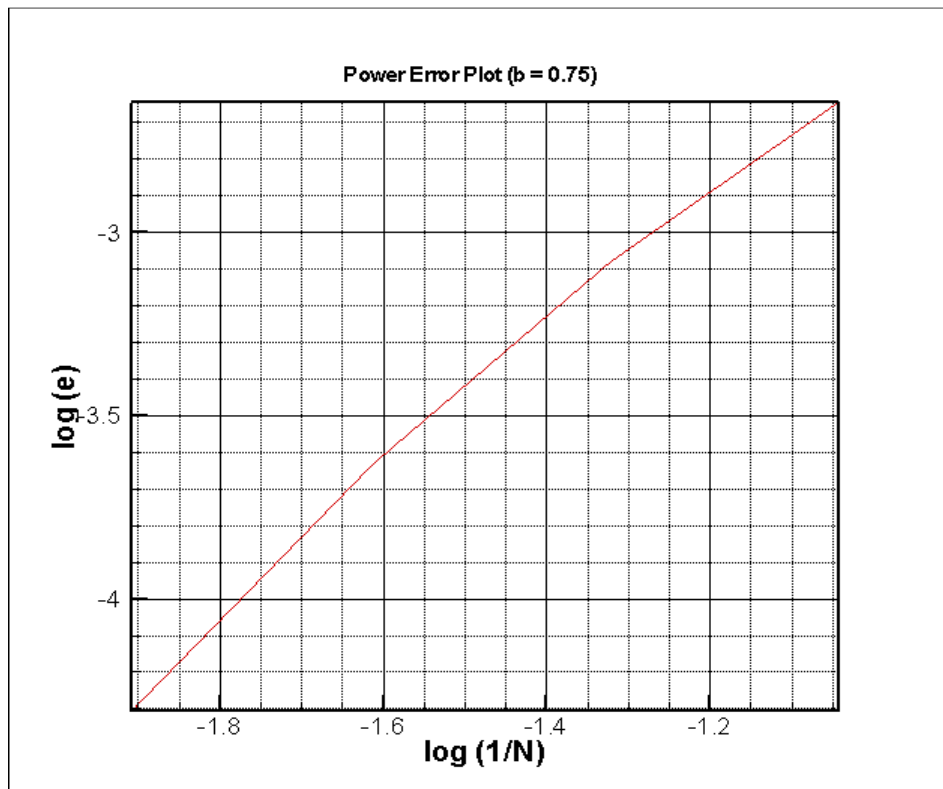
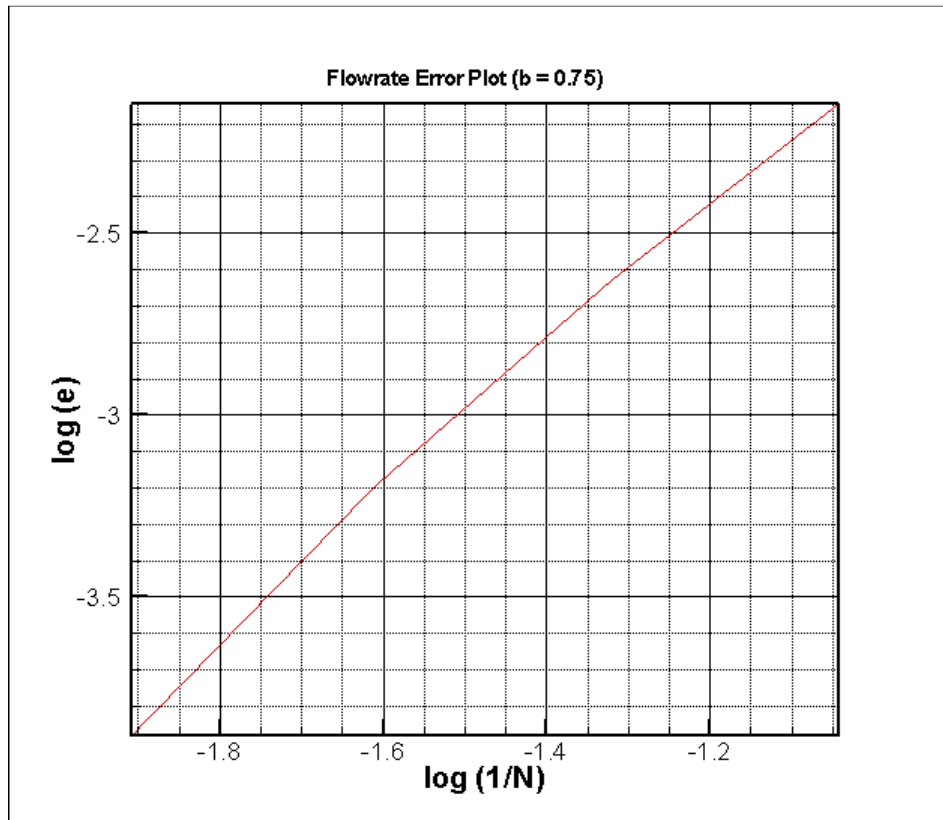


October 3, 2008

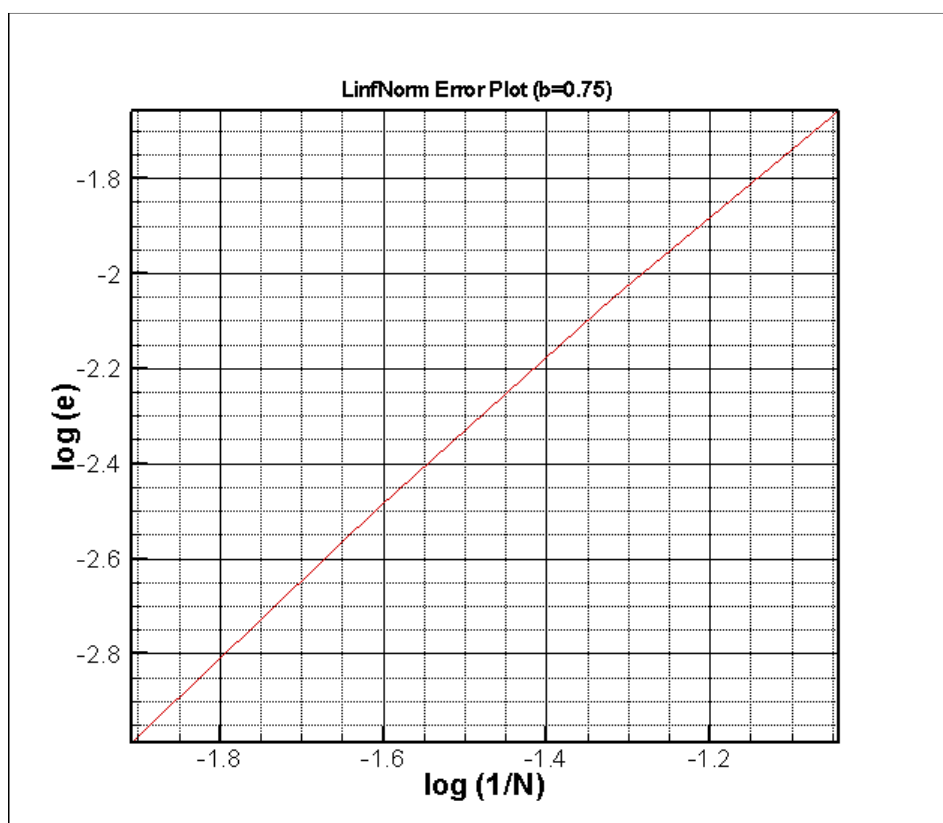
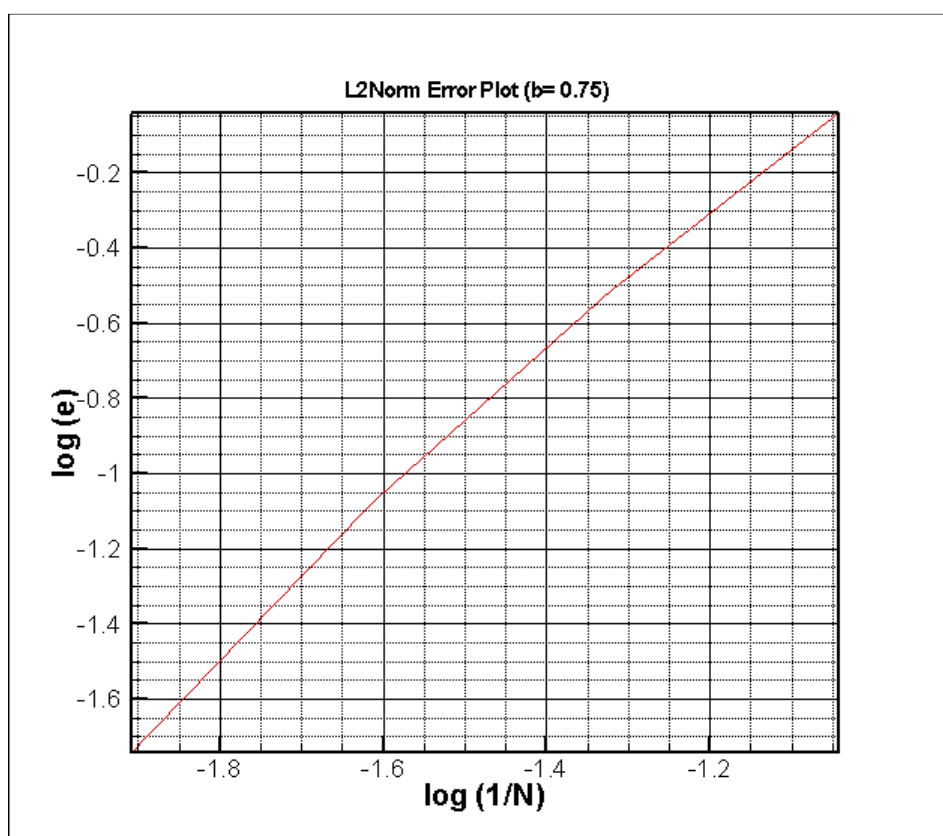


October 3, 2008

- $l=3.0, h=1.0, b=0.5$



October 3, 2008



October 3, 2008

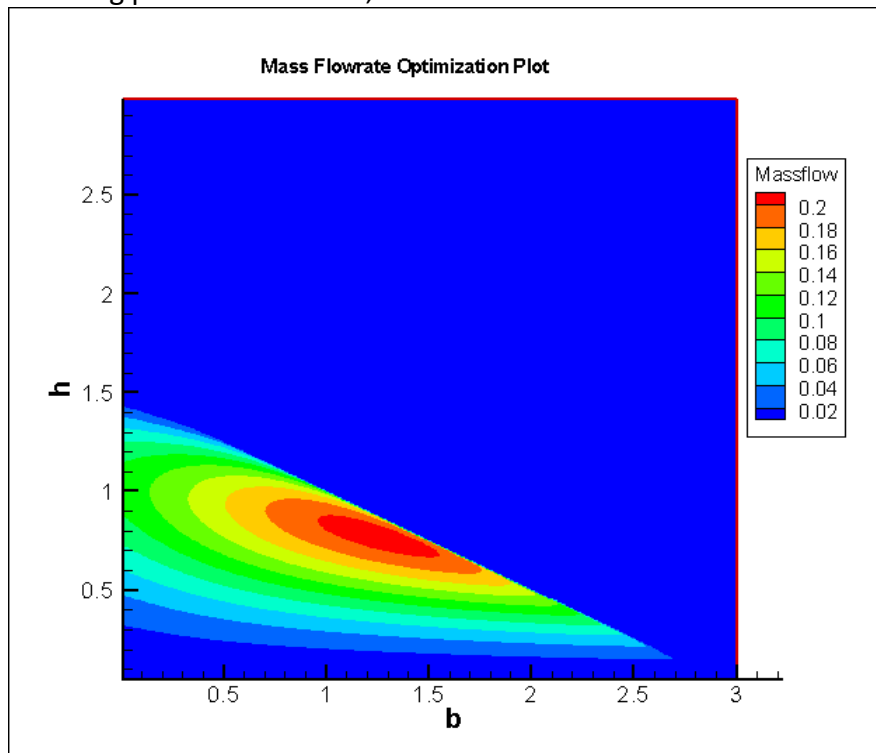
e) Finally, an optimization study was conducted with the available code to extract the maximum possible mass flow rate from the channel thus, specifying its dimensions in order to obtain this flow rate. In order to perform this optimization the constraint to the problem was identified as the 'a' specified in the problem statement.

$$a = \sqrt{\frac{(l-b)^2}{4} - h^2} \quad (5.0)$$

For any given 'b' and 'h' the parameter 'a' was identified to be non-negative and real. Hence using this constrain the solver was run for a range of b, and h values. The code was set up to sweep though 'b' values from 0 to 3 with step size of 0.01, for a fixed 'h'. On completion of which, the 'h' was varied for the next sweep and the range for 'h' was chosen from 0.05 (equal to the thickness, t, of the wall) to 3 with a step size of 0.01. During these sweeps the maximum Flow rate was extracted and the corresponding dimensions were specified. The following output for the maximum flow rate was obtained;

```
The Maximum Flow rate possible, Qmax=
0.209923070076135
The corresponding b,h, Power:
1.2700000000000000
0.7700000000000000
2.765081172350662E-002
```

Along with this a graphical optimization was also performed where the mass flow rate was plotted as a function of b and h which satisfy the constraint specified in equation 5.0 , and the following plot was obtained;

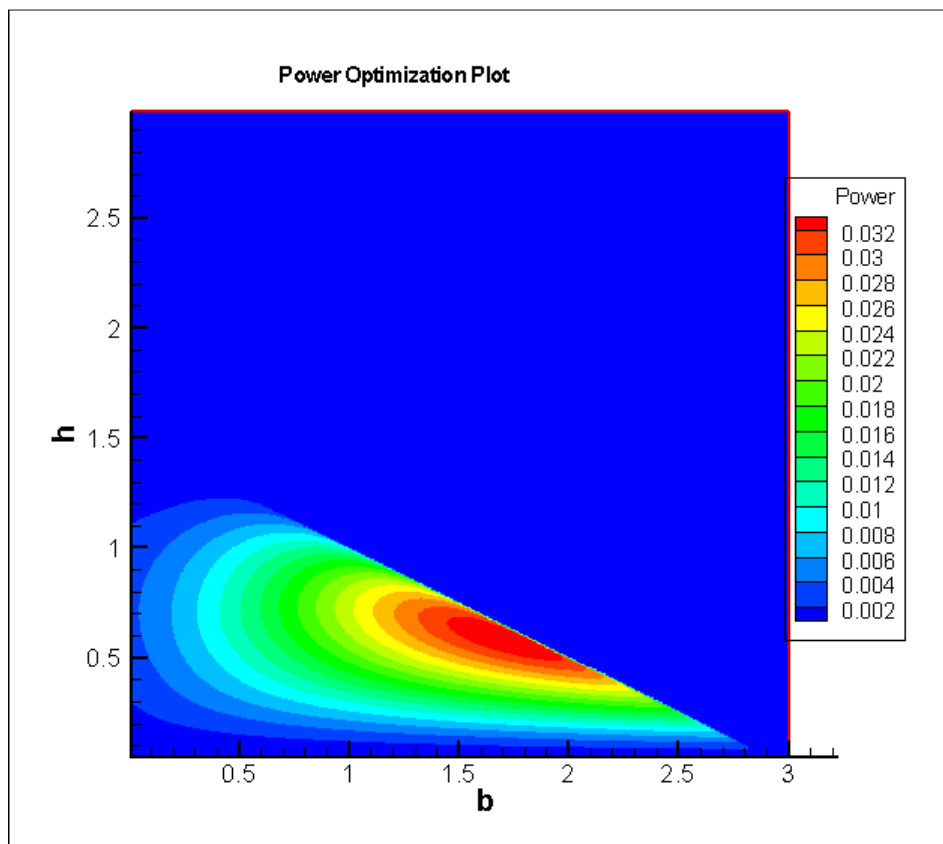


October 3, 2008

From the above plot the maximum flow rate was extracted using the probe function in Tecplot and the following values were obtained;

Maximum Flow Rate, $Q_{\max} = 0.209825$, $b = 1.26194$, $h = 0.775527$.

It should be noted that the above analysis can be improved to get better results by refining the sweep intervals of b and h . In order to obtain the above results a resolution of 0.01 in both b and h was used which can be refined for more accurate results. A similar graphical approach was used for the maximum power and the following plot for the maximum power was obtained;



From the above plot the maximum power was extracted using the probe function in Tecplot and the following values were obtained;

Maximum Flow Rate, $P_{\max} = 0.0338808$, $b = 1.70517$, $h = 0.591418$.

Hence, by comparing the two plots it can be concluded that the Maximum flow rate dimension may not correspond to the maximum power.

Bonus Question

The equation for the net, scaled, shear force on the channel walls and the integrated external force was given as follows;

$$F_{wall} = \int_{wall} \frac{\partial u}{\partial n} ds, \quad (6.0)$$

$$F_{ext} = \frac{1}{v} \int_{\phi} g \sin \alpha + \frac{\epsilon}{(y+t)^2} \quad (6.1)$$

In order to calculate the F_{ext} , an approach similar to the power and flowrate calculation was used to perform the integration.

Further, in order to calculate the F_{wall} , the unit normal to the south and east boundaries were calculated as follows;

For the south boundary;

$$(n_x, n_y) = (0, -1) \quad (6.2)$$

For the east boundary;

$$(n_x, n_y) = \left(\frac{2h}{l-b}, \frac{-2\sqrt{\left(\frac{l-b}{2}\right)^2 - h^2}}{l-b} \right) \quad (6.3)$$

This calculation was possible as the normals in this problem were constant as the edges were straight lines. The above calculation was done by using geometry. The governing equation for the wall was expanded as follows;

$$F_{wall} = \int_{wall} \frac{\partial u}{\partial x} n_x + \frac{\partial u}{\partial y} n_y ds, \quad (6.4)$$

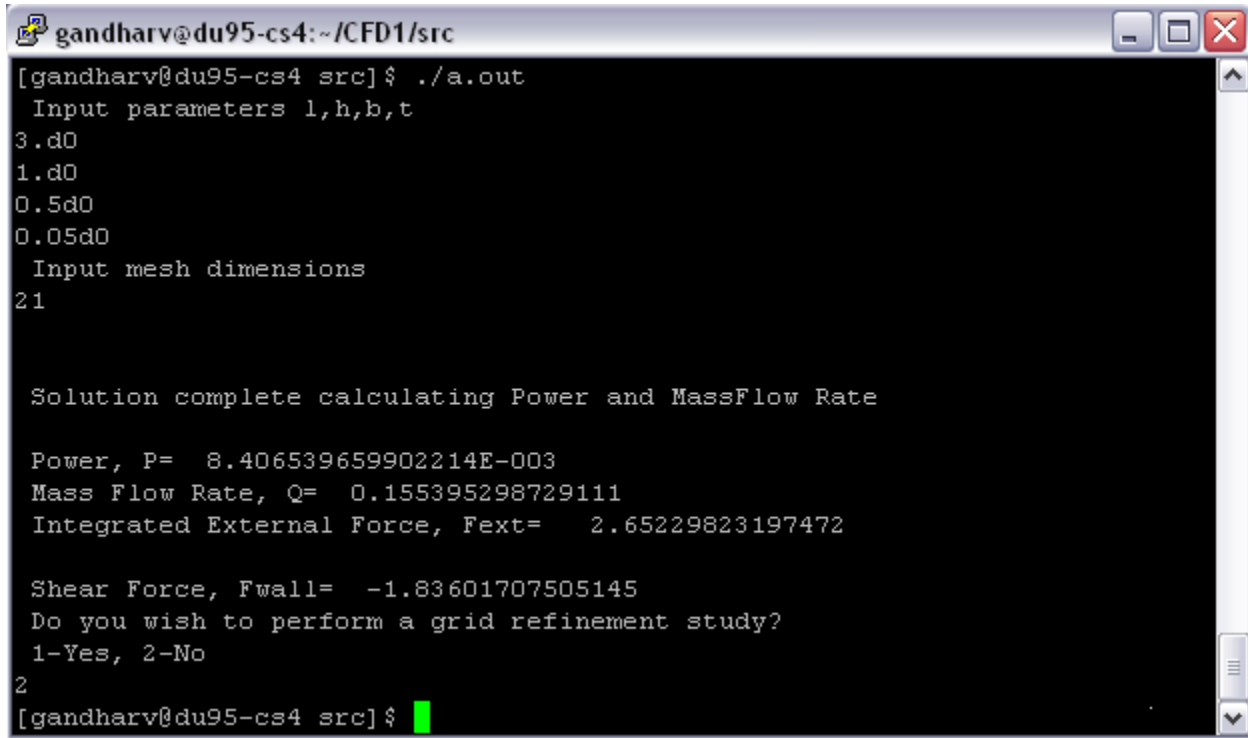
The derivatives were transformed to the computational domain and a finite difference scheme was applied at the south and east walls. At the interior points of the south and east boundaries a second order central difference combined with a one sided difference scheme was applied for the derivatives. This was integrated all around the boundaries and the results were recorded. The following values for the F_{wall} and F_{ext} were obtained;

N	41	81	161	321
F_{ext}	2.5534	2.5258	2.51862450555266	2.50842343593248
F_{wall}	-2.1174	-2.2644	-2.32254424809570	-2.38139826839670

From the above analysis it can be concluded that as the mesh is refined the two values for F_{wall} and F_{ext} approach the same value with opposite sign. From the physics of the problem it can be concluded that these two forces cancel each other which was demonstrated in this exercise.

Appendix

A sample screen shot of the validation case output from the program.



```
gandharv@du95-cs4:~/CFD1/src
[gandharv@du95-cs4 src]$ ./a.out
Input parameters l,h,b,t
3.d0
1.d0
0.5d0
0.05d0
Input mesh dimensions
21

Solution complete calculating Power and MassFlow Rate

Power, P= 8.406539659902214E-003
Mass Flow Rate, Q= 0.155395298729111
Integrated External Force, Fext= 2.65229823197472

Shear Force, Fwall= -1.83601707505145
Do you wish to perform a grid refinement study?
1-Yes, 2-No
2
[gandharv@du95-cs4 src]$
```

Works Cited

Hirsch, C. (2007). *Numerical Computation of Internal & External Flows*. John Wiley & Sons, Ltd.

John C. Tannehill, D. A. (1997). *Computational Fluid Mechanics and Heat Transfer*. Taylor & Francis.